Layered Fluid Structure and Anomalous Diffusion under Nanoconfinement

Gerald J. Wang and Nicolas G. Hadjiconstantinou*

Department of Mechanical Engineering, Massachusetts Institute of Technology, Cambridge, Massachusetts 02139, United States

ABSTRACT: Molecular diffusion under nanoconfinement can differ significantly from diffusion in bulk fluids. Using molecular dynamics simulations and molecular mechanics arguments, we elucidate the effect of layering at the confining boundaries on the self-diffusion of a simple, single-phase, confined fluid. In particular, we show that anomalous diffusion due to layering is controlled by the degree of layering as quantified by the recently proposed Wall number (Wa), which compares the strength of the wall−fluid interaction to the thermal energy. For low Wall numbers, layering is not sufficiently pronounced so as to have a significant effect, whereas for $Wa \gtrsim 1$, layering is sufficiently important to have a significant effect on diffusion dynamics. In the latter regime, we find that fluid in the fluid−solid interfacial region tends to exhibit restricted dynamics and may only leave this region via a thermally activated hopping process. We also identify conditions under which diffusivity under confinement can be estimated, to a good approximation level, as a weighted average of the bulk and first-layer region diffusivities, leading to direct expressions quantifying the deviation from bulk behavior in terms of the confinement length scale.
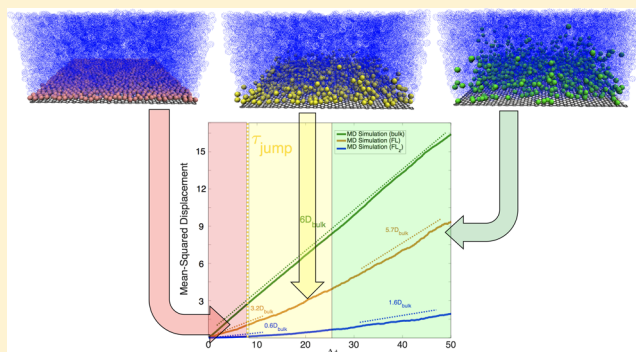
INTRODUCTION

Fluids can exhibit a wide range of anomalous properties when placed under nanoscale confinement.[1−5] These anomalies typically result from the increasing importance of surface effects relative to bulk effects as the confinement becomes more pronounced. One especially notable phenomenon is that of anomalous diffusion, namely, the observation that the diffusive behavior of fluids under nanoconfinement may differ significantly from their bulk counterparts. This phenomenon has been observed in a wide range of fluid simulations, including simulations of hard-disk/sphere fluids,[6−9] Lennard-Jones (LJ) fluids,[6,10−13] water,[14−16] oxygen,[17] and a wide variety of alkanes,[18] as well as many experimental measurements.[19−21]

Anomalous diffusive behavior is of great engineering interest in applications involving nanoscale fluid transport, such as nanoscale desalination membranes,[22] nanoscale drug delivery,[23] or chemical transport through zeolites.[24] In general, diffusion plays a dominant role in mass transfer for systems with small pore radii where it may be challenging to impose pressure gradients that are sufficiently large to drive convection. Studying equilibrium diffusion in nanoscale systems also sheds light on transport within these systems, by way of the fluctuation-dissipation relations that connect equilibrium and transport quantities. This approach has been fruitfully pursued in the literature, as reviewed in ref 25.

In this work, we establish quantitative connections between anomalous diffusion and the layered structure of fluid near a confining boundary as quantified by the Wall number, first introduced in ref 26, which serves as a measure of the relative importance of fluid−wall interaction and thermal effects. Here, we note that although the spatial dependence of diffusivity has been studied before from a thermodynamic point of view,[8,9,27] the present work provides a different perspective by (a) focusing on a model that provides measures of the diffusion coefficient (as a function of nanoconfinement) that are directly relatable to the mean-squared displacement and (b) taking into account, for the first time, the degree of layering at the fluid−solid interface.

BACKGROUND AND OBJECTIVES

We begin by considering the structure of a simple fluid of average density ρ_{ave}^* and temperature T^* confined within a rigid graphene nanoslit of width L^*. For our purposes, interatomic interactions are governed by the Lennard-Jones (LJ) potential[28]

$$V^*(r^*) = 4\varepsilon^* \left[\left(\frac{\sigma^*}{r^*} \right)^{12} - \left(\frac{\sigma^*}{r^*} \right)^{6} \right] \tag{1}$$

where parameters ε^* and σ^* denote the interactions between a fluid particle and a wall atom. Each fluid molecule has mass m^*. Throughout this work, asterisks indicate dimensional quantities. Nondimensional quantities, which do not carry asterisks, are scaled by the length scale σ^*, energy scale ε^*, time scale $\sqrt{m^*\sigma^{*2}/\varepsilon^*}$, temperature scale ε^*/k_B, and diffusivity scale $\sqrt{\varepsilon^*\sigma^{*2}/m^*}$, where k_B is Boltzmann's constant. Our molecular-

dynamics (MD) simulation methodology is described in detail in the Appendix.

In previous work,[26] the authors have shown that the presence of layering at a fluid–solid interface in a simple fluid is controlled by the Wall number, $Wa \equiv n/T$, where n is the areal density of solid atoms in the wall and T is the temperature (we emphasize here that these are both dimensionless quantities). The Wall number, compares the relative importance of the energy scale of fluid–solid interaction (which is proportional to the wall density) and the thermal energy scale, provided that the system has a finite energy scale for fluid–solid interactions. In particular, when $Wa \ll 1$, the "randomness" associated with high thermal background means that the fluid density near the wall will not exhibit strong inhomogeneities; otherwise, if Wa is not much less than 1 (i.e., $Wa \gtrsim 1$) we expect distinct fluid layering to form. In general, whether or not pronounced layering exists, the minimum separation between the wall and the fluid has been calculated as $z_{min} = (2/5)^{1/6}$ for both the planar wall geometry as well as the cylindrical nanopore geometry.[5,26] This quantity is illustrated on a representative spatial density profile for layered fluid in Figure 1, obtained
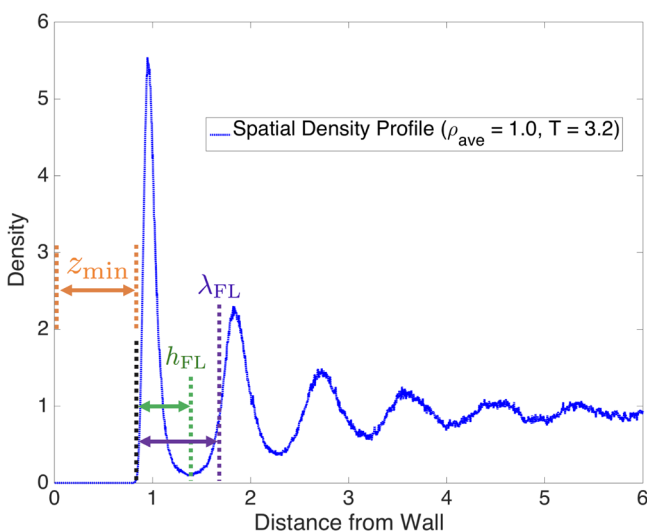

Figure 1. Fluid density (relative to the channel-averaged density, $\rho_{ave} = 1.0$) as a function of distance from the wall. This representative profile shows key features of fluid layering near the fluid–solid interface at high Wall number ($Wa = 1.2$). The minimum separation z_{min} is marked in orange, the first-layer width h_{FL} is marked in green, and the first-layer wavelength λ_{FL} is marked in purple.

from MD simulation. The figure also highlights h_{FL}, the width of the fluid layer closest to the fluid–wall interface, which we will refer to as the "first fluid layer". For a LJ fluid in the range $2 \leq T \leq 20$ and $0.4 \leq \rho_{ave} \leq 1.2$, h_{FL} has been shown[26] to be predominantly a function of density and well approximated by

$$h_{FL} = 0.80 - 0.30\rho_{ave} \tag{2}$$

In the present work, we show how the above characterization can be used to provide new insights into the connection between wall–fluid interaction and diffusion under nano-confinement. To begin, we expect that when layering is not very significant, i.e., when $Wa \ll 1$, the diffusion coefficient will be, to a good approximation level, unaffected by fluid layering. This is in agreement with previous work by Mittal et al.[11] in which the diffusion of a LJ fluid under confinement was found to obey, to a good approximation level, the same excess-entropy

relation as the bulk (unconfined) fluid. These results can be understood by noting that in ref 11 the LJ fluid was confined by a 9–3 LJ wall potential of the form

$$V(z) = \frac{2}{15}z^{-9} - z^{-3} \tag{3}$$

which has an effective number density $n = 3/(2\pi)$ (compare to eq (5.9.2) in ref 29), leading to an effective Wall number range of $3/(20\pi)-3/(2\pi)$ (the authors in ref 11 considered temperatures in the range $1 \leq T \leq 10$).

On the other hand, for $Wa \gtrsim 1$, we expect the particle dynamics within the layered structure shown in Figure 1 to be different than that in the bulk (both due to the different fluid density and due to dimensional restriction), resulting in an overall diffusion coefficient that is different from the bulk (when the system size is not much larger than the characteristic layering length scale). Given that the effect of the first fluid layer is the most pronounced, to make our discussion as quantitative as possible, we will focus on systems that feature at most one well-defined fluid layer. A single-layer-forming system exhibits strong fluid layering due to the (highly ordered) solid surface but weak subsequent fluid layering due to this (only somewhat ordered) fluid layer. This notion can be made rigorous by defining a secondary Wall number, $Wa_{FL} \equiv \sum_{FL}/T$, where $\sum_{FL}$ is the areal density of molecules within the first fluid layer. This secondary Wall number quantifies the degree to which the first layer induces a second fluid layer. Thus, the single-layer-forming regime is defined by the simultaneous conditions $Wa \gtrsim 1$ and $Wa_{FL} \ll 1$. We note that in general $\sum_{FL} = \sum_{FL}(\rho_{ave}, T)$; earlier work in ref 26 suggests that single-layer-forming systems are common at typical temperatures and densities of engineering interest.

■ RESULTS AND DISCUSSION

Preliminary Observations. In this section, we discuss a number of observations and simulation results that are important for subsequent results in this work.

Particle Residence Time within the First Layer. As would be expected, in single-layer-forming systems at equilibrium, the average mass of fluid within the first layer is statistically constant. However, the particles within that layer are in constant exchange with particles from the bulk, an observation first reported in ref 30. This motivates the definition of a jumping time scale τ_{jump}, which characterizes the time for turnover of the fluid content in the first layer. In particular, we define τ_{jump} to be the average time it takes a fraction e^{-1} of the first-layer fluid molecules to exchange with the bulk. We propose that hopping between the first-layer region and the bulk is a Kramers-type thermally activated process, which implies[31]

$$\tau_{jump} \sim \exp\left(\frac{\Delta U^*_{barrier}}{k_B T^*}\right) \tag{4}$$

and since $U^*_{barrier} \sim n^* \sigma^{*2} \varepsilon^*$, we deduce that

$$\tau_{jump} \sim \exp\left(\frac{n^* \sigma^{*2} \varepsilon^*}{k_B T^*}\right) \sim \exp(Wa) \tag{5}$$

where the last proportionality follows from the definition of the Wall number. We note that here we neglect the possible ρ-, n- and T-dependence of prefactors in this proportionality.

We verify this prediction by extracting the jumping time scale from MD simulations. Values of τ_{jump} for a variety of Wall numbers and average fluid densities are shown in Figure 2.
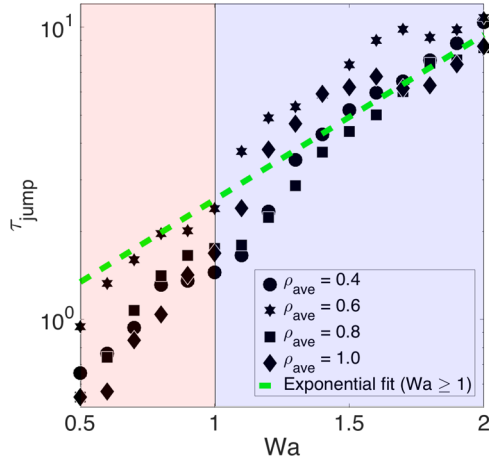

Figure 2. Characteristic time τ_{jump} taken by fluid molecules to leave the first layer is shown as a function of the Wall number (simulations performed by varying T at fixed n). The blue color ($Wa \geq 1$) indicates the region over which the exponential fit is based. For all densities, τ_{jump} is increasing in Wa; in particular, the exponential fit for layer-forming systems indicates that particle escape from a well-formed fluid layer is consistent with a thermally activated hopping mechanism.

Here, we note that the different values of the Wall number were generated by varying the temperature for a fixed wall structure (n). We find that there is an exponential relation between the jumping time scale and the Wall number, which supports the proposed mechanism.

Spatially Resolved Diffusivity. We compute the three-dimensional (3D) diffusivity within some spatial region R using the relation

$$D_R = \frac{1}{N_R} \sum_{i=1}^{N_R} \frac{(\Delta \mathbf{r}_i)^2}{6\Delta t} \tag{6}$$

where $\Delta \mathbf{r}_i$ is the three-dimensional displacement of the i-th particle and $\Delta t = t_f - t_0$. Here, t_f is the time at which the final sample is recorded and t_0 denotes the sampling start time (when all N_R particles over which the averaging is performed were located in region R). This expression will be used to calculate the diffusion coefficient in the first layer (denoted by the subscript "FL"), the bulk (denoted by the subscript "bulk"), and the entire system (denoted by the subscript "all").

Characteristic Time Scales. It is well known[32] that confinement can have a large effect on the diffusion coefficient. Specifically, given a uniformly distributed set of particles confined in a slab of characteristic size L, the mean-squared displacement in the direction normal to the boundaries (z) averaged over all initial particle positions is given by[10]

$$\langle \Delta z^2 \rangle = \frac{L^2}{6} - \frac{16L^2}{\pi^4} \sum_{j=1}^{\infty} (2j-1)^{-4}$$

$$\exp(-(2j-1)^2 \pi^2 Dt/L^2) \tag{7}$$

From this expression, we can see that the traditional result, $\langle \Delta z^2 \rangle = 2Dt$, is valid for times that are very short compared to the diffusion time based on the system length scale ($t \ll \tau_L = L^2/(\pi^2 D)$). For times on the order of or longer than τ_L, $\langle \Delta z^2 \rangle$

$\to L^2/6$. In other words, for a fluid confined in a nanoslit of gap height L, $\lim_{t \gtrsim \tau_L} \langle (\Delta \mathbf{r})^2 \rangle \to 4Dt + L^2/6$.

Because of the quadratic dependence of τ_L on L, accessing times much longer than τ_L using molecular simulation is computationally expensive unless the system is small. As a result, studies of anomalous diffusion have typically investigated times that are not large compared to τ_L and are thus reporting diffusion coefficients that do not reflect the dimensional confinement, namely $\langle (\Delta \mathbf{r})^2 \rangle = 6Dt$. This, however, is not to be confused with bulk diffusion since, due to fluid layering, the coefficient of diffusion is spatially variable within the fluid domain, i.e., $D \neq D_{bulk}$. To be more specific, fluid in the first fluid layer can be at a different density than the bulk;[26] additionally, because the first layer thickness is less than σ, fluid in the first layer is for all practical purposes dimensionally restricted for all times.

In the interest of consistency with previous work, the diffusion coefficient reported and modeled here corresponds to time scales $t \ll \tau_L$ for which the bulk of the system is not dimensionally restricted. This approach is sufficiently general because in addition to providing a model for the coefficient of diffusion for these time scales, it includes all of the ingredients needed for obtaining the diffusion coefficient for all times via 7.

We will quantify the effect of the first fluid layer by measuring the diffusion coefficient using the definition in 6, for an observation period that is sufficiently short ($\Delta t = 0.5\,\tau_{jump}$) such that the number of particles that leave the layer is small. By restricting the averaging process to this time window and to particles within the first layer at the initial time t_0, we effectively restrict the averaging process to particles that reside within the first layer during the averaging process; this ensures that this measurement captures the dynamics specific to the first-layer region and can thus be used to represent the first-layer contribution over time intervals of arbitrary duration (in equilibrium, particles leaving the first layer are replaced by others traveling in the opposite direction, resulting in a statistically steady first-layer population). Although τ_{jump} is a molecular time scale, for layer-forming systems ($Wa \gtrsim 1$), it is sufficiently longer than the time over which the first fluid layer is dimensionally restricted (τ_{FL}), which is of order less than unity; to see that $\tau_{FL} < 1$, we note that characteristic diffusivities are $O(10^{-1})$, while characteristic layer widths are smaller than unity (see 2). In other words, sufficient time scale separation exists for Δt to satisfy both $\Delta t \gg \tau_{FL}$ and $\Delta t < \tau_{jump}$ when measuring diffusion in the first layer. Because of the former condition, our data analysis neglects the small effect of τ_{FL}; in other words, sampling starts at t_0 instead of $t_0 + \tau_{FL}$. We also note, in the same vein, that we have verified that the very short time τ_b over which motion is ballistic[33] can also be safely neglected ($\tau_b \ll \Delta t$).

These considerations are highlighted in Figure 3, which compares the various time scales that are important in this problem.

Layering and Anomalous Diffusivity. We turn our attention now to the role of layering in anomalous diffusivity. As explained in the previous section, we expect the effect of layering to be small for $Wa \ll 1$ and thus we focus on the regime $Wa \gtrsim 1$. The basic idea behind the analysis that follows is that, for practical purposes, the diffusion coefficient of the confined fluid is the aggregate of two main contributions: the fluid within the two first layers (one layer at each confining boundary) and the fluid in the remainder of the system (which
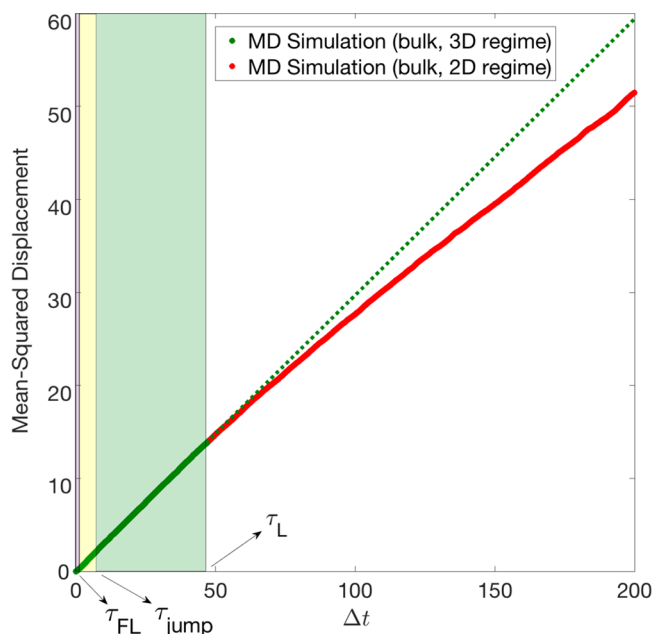
Figure 3. Mean-squared displacement vs time for particles in the bulk region ($L = 15$) obtained from MD simulation. For $\Delta t \gtrsim \tau_{\mathrm{L}} = 0.1 L^2 / (\pi^2 D_{\mathrm{bulk}})$, the bulk fluid enters the "two-dimensional regime" as it begins to exhibit confinement effects associated with the finite-sized channel. Note that the transition regime associated with τ_{FL} (shown in purple) is significantly shorter than that associated with τ_{jump} (shown in yellow), which is in turn much smaller than the "3D regime" (shown in green). As a guide to the eye and to emphasize that the MD result deviates from the bulk 3D behavior, the bulk 3D line is extended beyond the 3D regime by the green dotted line.

we will refer to as the bulk region). Assuming that the diffusion coefficient of the fluid in the bulk region is equal to the unconfined fluid value (at the same thermodynamic conditions), the challenge lies in describing the diffusion coefficient of particles in the first layer.

First Layer as a "Dimensionally Restricted" Fluid. We begin by considering semi-infinite systems. In our simulations, we have taken $L = 30$, which in practice is sufficiently large. Given the activated nature of their escape, we consider first-layer molecules to comprise a dimensionally restricted fluid (while residing in the first layer) exhibiting standard Fickian diffusion in two dimensions (as opposed to three dimensions in the bulk); this restriction in dimension is expected to reduce the diffusivity by a factor of a third. We further note that this layer is of considerably higher density than the bulk[26] and that it is well known for diffusivity to decrease with increasing fluid density.[34] As a consequence, we expect the following estimate

$$D_{\mathrm{FL}} \leq \frac{2}{3} D_{\mathrm{bulk}} \qquad (8)$$

to serve as a reliable approximate upper bound to the diffusivity of first-layer molecules.

This bound is illustrated in Figure 4, which shows the mean-squared displacement for various groups of molecules as a function of time. Here, we emphasize again that although our interest lies in characterizing the fluid in an Eulerian fashion, that is, characterizing the first fluid layer and bulk regions separately, it is sometimes more convenient to achieve this characterization by studying the Lagrangian dynamics of molecules in the $\Delta t \ll \tau_{\mathrm{jump}}$ and $\Delta t \gg \tau_{\mathrm{jump}}$ limits, respectively. The figure shows that the diffusivity in the first-layer region is
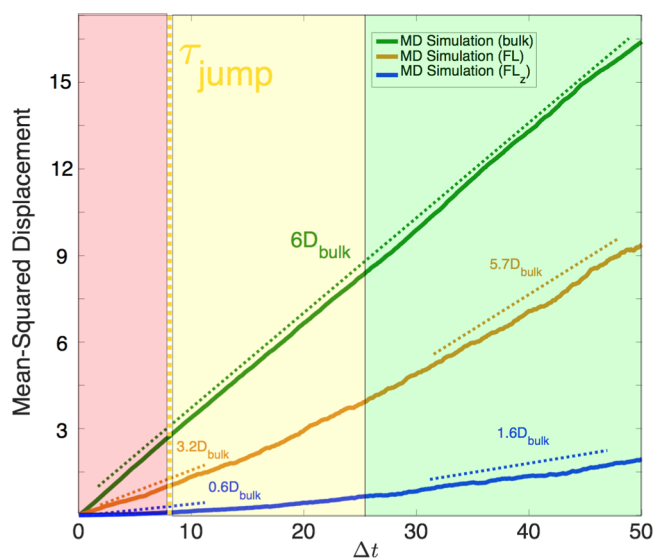

Figure 4. Mean-squared displacement as a function of time for particles within the bulk (dark green line), for particles within the first layer (orange line), and for the z-component of particles in the first layer (blue line). Note the difference in slopes between $\Delta t \lesssim \tau_{\mathrm{jump}}$ (the dimensionally restricted and transition regimes, shaded in red and yellow, respectively) and $\Delta t \gg \tau_{\mathrm{jump}}$ (the "dimensionally unrestricted" regime, shaded in green).

considerably smaller than in the bulk for times $\Delta t \ll \tau_{\mathrm{jump}}$ (insufficient time for molecules to escape to the bulk). However, as Δt increases beyond τ_{jump} (i.e., there has been significant turnover between the first-layer region and the bulk region), we observe that the diffusive behavior of the group of molecules that began in the first-layer region begins to approach the bulk behavior. In particular, we find that the contribution of the wall-normal component for this group of molecules is much closer to a third of the fluid's bulk diffusivity as compared to the early time regime. This demonstrates the lifting of the dimensional restriction once sufficient time has passed for first-layer molecules to move into the bulk region. We emphasize that this pronounced difference between the first-layer region and the bulk region will only occur provided that Wa is not much less than 1.

Anomalous Diffusivity Magnitude. To quantify the degree to which layering induces anomalous diffusive effects, we introduce the diffusivity ratio Q, defined as the ratio of the overall diffusivity to the diffusivity of fluid molecules within the bulk region

$$Q = \frac{D_{\mathrm{all}}}{D_{\mathrm{bulk}}} \qquad (9)$$

By construction, Q approaches unity in the limit that all fluid molecules in the system exhibit bulk behavior. We therefore expect that in a system with no layering there should be no appreciable deviations of Q from unity. On the other hand, in a single-layer-forming system, we expect $Q < 1$, since the first layer experiences significant dimensional restriction. In Figure 5, we demonstrate that these regimes can clearly be observed within MD simulations.

Confinement-Induced Anomalous Diffusivity. On the basis of our previously stated assumption that all fluid particles outside the first-layer region exhibit the bulk diffusivity, whereas the diffusivity within the first layer is assumed constant at the value D_{FL}, the overall diffusion coefficient can be written[10] as
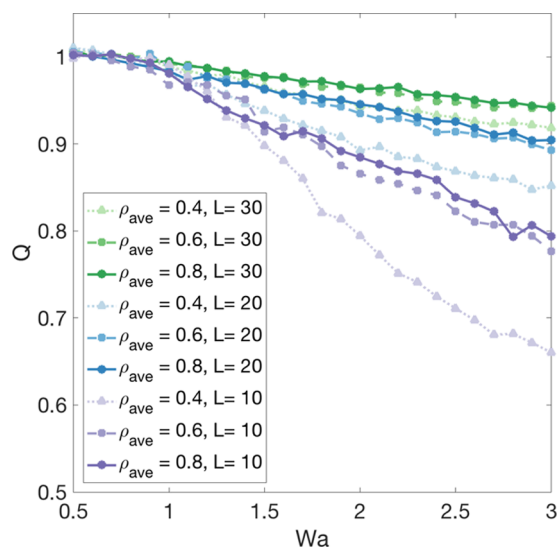
Figure 5. Diffusivity ratio Q as a function of the Wall number for a variety of densities and channel widths. Note that in the low-Wa regime, $Q \approx 1$ for all densities and channel widths; in the high-Wa regime, Q can be considerably less than unity.

Figure 6. Diffusivity ratio Q as a function of confinement length scale L for systems in the layering regime, $Wa \geq 1$ ($\rho_{ave} = 0.8$). The colors run from white ($Wa = 1.0$) to blue ($Wa = 3.0$). The inset shows the diffusivity anomaly for several systems in the low-Wa regime ($0.2 \leq Wa < 1.0$).

the weighted average of bulk particles contributing D_{bulk} and first-layer particles contributing D_{FL}, leading to

$$D_{all} = D_{bulk}\left(1 - 2\frac{C(\rho_{ave}, T)h_{FL}(\rho_{ave})}{L}\left(1 - \frac{D_{FL}}{D_{bulk}}\right)\right) \quad (10)$$

where $C(\rho_{ave}, T) \equiv \rho_{FL}/\rho_{bulk}$ reflects the enhanced fluid density within the first layer and the factor of 2 comes from the presence of a first layer at each of the two confining walls. Here, ρ_{FL} refers to the density of fluid within the first layer; specifically, it is defined as $\rho_{FL} \equiv N_{FL}/(Ah_{FL})$ where N_{FL} is the number of fluid molecules in the first layer and A is the fluid–solid interfacial contact area. Alternatively, ρ_{FL} may be written as $\sum_{FL}/h_{FL}$, where $\sum_{FL}$ is the areal density of fluid within the first layer. A detailed treatment of these length and density scales is presented in ref 26.

Based on the observation that diffusion within the first-layer region is much slower than in the bulk region, we can neglect the contributions of the first-layer region to obtain a simple lower bound on the diffusivity ratio as

$$Q_{min} = 1 - 2\frac{C(\rho_{ave}, T)h_{FL}(\rho_{ave})}{L} \quad (11)$$

Similarly, given the upper bound in 8 for diffusivity within the first layer, we can approximately bound the diffusivity ratio from above by

$$Q_{max} = 1 - \frac{2}{3}\frac{C(\rho_{ave}, T)h_{FL}(\rho_{ave})}{L} \quad (12)$$

The lower bound 11 is theoretically valid for all Wall numbers, since $D_{FL} \geq 0$ is always true. On the other hand, the upper bound is limited to $Wa \gtrsim 1$; even then it is only approximately valid since D_{FL} can exceed $\frac{2}{3}D_{bulk}$ due to the small but nonzero contribution to the diffusivity from motion in the wall-normal direction (see Figure 4).

These predictions are validated in Figure 6. In particular, regardless of Wall number, all systems exhibit diffusivity ratios that are bounded below by Q_{min}. For $Wa \geq 1$, there is a strictly
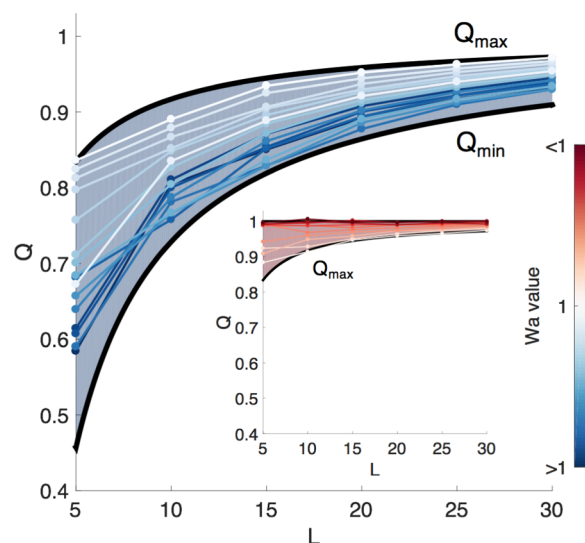
increasing relationship between the diffusivity ratio and the confinement length scale. This is because a greater proportion of fluid is contained within the first-layer region as the channel width decreases. In all of these systems, the diffusivity anomaly is found to be bounded from above by Q_{max}. In contradistinction, for $Wa < 1$, the diffusivity anomaly is close to unity (within 12% for all simulated cases) regardless of the channel width. As expected, when $Wa < 1$, Q can exceed Q_{max}, which serves as an upper bound on Q only for $Wa \gtrsim 1$. This indicates that the presence of the confining boundary is negligible, which is expected since there is little layer formation in the low-Wa regime. As such, we emphasize that 12 is not a strict upper bound, and it may be violated in systems where a sufficiently pronounced first layer does not form.

Model for the Anomalous Diffusivity in the First Layer. The above results have validated that a system's overall diffusivity can be expressed as a linear combination of bulk and layer contributions, namely, as described by 10, and that reliable bounds for the overall diffusivity of the confined fluid can be derived on the basis of physical arguments. Unfortunately, D_{FL} is not known in general and so far we have relied on bounds for this quantity, which constrain the diffusivity anomaly over a wide range of simulation length scales. Developing a model for D_{FL} would allow precise, predictive calculation of $D_{all} = D_{all}(L)$.

In this section, we propose an approximation that allows calculation of D_{FL} to a reasonable accuracy level using already known information. This approach, motivated by the findings of Mittal et al.,[11] makes the assumption that, other than the dimensional restriction, the diffusivity of the fluid in the first layer is related to its density in the same fashion as the bulk fluid. In other words, we take

$$D_{FL} = \frac{2}{3}D_{bulk}(\tilde{\rho}_{FL}, T) \quad (13)$$

where $D_{bulk}(\rho, T)$ is the diffusion coefficient of the bulk LJ fluid as a function of density and temperature. Here, $\tilde{\rho}_{FL}$ is defined as N_{FL}/λ_{FL}, where λ_{FL} is a length scale empirically determined to provide reasonable results. In particular, λ_{FL} is defined as the
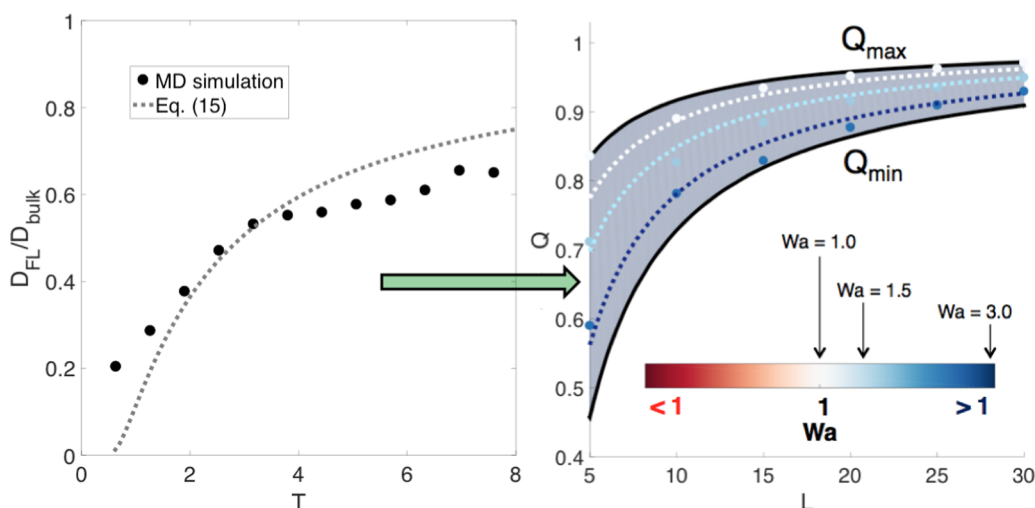
Figure 7. On the left, the ratio of first-layer diffusivity to bulk diffusivity as a function of temperature ($\rho_{ave} = 0.8$). The dots indicate measurements directly from MD simulation via measurements of mean-squared displacement, as given in 6; the solid line shows 15. On the right, the diffusivity anomaly as a function of the confinement length scale using the values of D_{FL}/D_{bulk} calculated via 10 and 14; these predicted values are in good agreement with the MD results shown in Figure 6 for a variety of $Wa \geq 1$.

distance between z_{min} and the point at which the fluid density profile attains a value halfway between its second trough and peak, as shown in Figure 1.

For the systems of interest here ($L \gtrsim 5$), 10 does not require D_{FL} to be determined to great accuracy because the contribution of the bulk region is typically comparable to or larger than that of the first fluid layer. In other words, even an estimate for D_{FL} leads to a reasonably accurate prediction for D_{all}. Therefore, in the interest of simplicity, we approximate $D_{bulk}(\rho, T)$ by the diffusivity of a bulk hard-sphere gas (see ref 11 for a discussion of how the Lennard-Jones diffusivity approaches the hard-sphere result in the limit of high temperature). In particular, we use the simple relationship due to Heyes[35]

$$D_{bulk} T^{-1/2} = 0.212 \rho_{bulk}^{-1} - 0.260 + 0.080 \rho_{bulk} \qquad (14)$$

This result immediately leads to the following expression for calculating the ratio D_{FL}/D_{bulk} needed in 10

$$\frac{D_{FL}}{D_{bulk}} = \frac{2}{3} \frac{0.212 \tilde{\rho}_{FL}^{-1} - 0.260 + 0.080 \tilde{\rho}_{FL}}{0.212 \rho_{bulk}^{-1} - 0.260 + 0.080 \rho_{bulk}} \qquad (15)$$

This expression is in reasonable agreement (less than 20% error, for most simulated temperatures) with the values of D_{FL}/D_{bulk} measured using 6, as shown in Figure 7.

Figure 7 also shows that we can use 15 to fill in the previously unknown term in 10, thereby obtaining reasonably accurate predictions for the diffusivity anomaly as a function of the confinement length scale.

■ CONCLUSIONS

Simple fluids under nanoconfinement can exhibit a range of highly modified diffusive behaviors. Through a combination of molecular-mechanics arguments and MD simulations, we have shown how the complex dependence of diffusivity on the nondimensional temperature, density, as well as confinement length scale, can be explained using recent developments in the understanding of layering at the fluid–wall interface. In particular, we have shown that for sufficiently weak layering, as characterized by the Wall number, the diffusion coefficient is

not significantly perturbed from its bulk value, as seen in a number of previous studies. On the other hand, the layered fluid structure that forms in systems at high Wall number exhibits diffusive behavior that can be considerably slower than diffusion far away from the interface. In highly confined systems, where the fraction of fluid contained within the layered regions is appreciable, the suppressed diffusion within the first layer leads to an anomalously low overall diffusion coefficient. We have provided bounds that can be computed accurately and rapidly, without the use of MD simulation, to estimate the magnitude of the diffusion anomaly in our model system. We have also shown that the overall diffusivity anomaly as a function of the confinement length scale can be approximately calculated in closed form by approximating the first-layer diffusivity as the bulk diffusivity at the first-layer density. The length scale (layer width) used to define this density has been empirically determined.

As stated in the discussion of characteristic time scales, the overall diffusion coefficients given here are applicable to times given by $t \ll \tau_L$, i.e., sufficiently short, that the bulk fluid is not dimensionally restricted. If the overall diffusion coefficient for $t \gtrsim \tau_L$ is needed, then D_{bulk} needs to be replaced by $2D_{bulk}/3$ in 10. We also note that the overall diffusion coefficient provided here averages over the spatial and directional distribution of diffusion rates exhibited in this problem. In cases where the diffusion rates in specific directions are of interest, they can be directly obtained for $t \ll \tau_L$ as $D_{bulk}/3$ for each dimension in the bulk and $D_{FL}/2$ in each of the in-plane directions within the first layer. For $t \gtrsim \tau_L$, the bulk diffusion is reduced to $D_{bulk}/3$ for each of the slit in-plane directions and zero in the slit transverse direction.

It is worth noting that these results, obtained for a simple fluid, are also expected to apply to more-complex fluids, such as water. For example, it has been shown that the diffusive behavior of water confined within a carbon nanotube exhibits a dependence on the confinement length scale.[36] By establishing the relationship between confined fluid structure and anomalous diffusivity, this study lays the groundwork for one potential mechanism to tune nanofluidic mass transport by engineering the fluid–solid interface.

APPENDIX: MOLECULAR-DYNAMICS SIMULATIONS

In this work, graphene was modeled as a sheet of carbon atoms packed in a hexagonal lattice with side length of 1.421 Å. To minimize edge effects, each graphene sheet measured at least 31 by 31 in the in-plane directions. For semi-infinite systems, the channel width was $L = 30$.

Interactions between carbon and fluid were modeled using $\sigma^* = 3.15$ Å and $\varepsilon^* = 0.15$ kcal mol^{-1}, whereas fluid–fluid interactions were modeled using $\sigma_f^* = 3.15$ Å and $\varepsilon_f^* = 0.15$ kcal mol^{-1}. A cut-off distance of $4\sigma^*$ was used throughout.

Simulations were conducted in LAMMPS[37] in the NVT ensemble using a Nosé–Hoover thermostat[38,39] within the range of densities $0.4 \leq \rho_{ave} \leq 1.0$. The majority of simulations were conducted within $2 \leq T \leq 18$. The simulation time step was 6.25×10^{-4}. Each system was allowed to equilibrate for a time of 4, after which samples were recorded every 1.25×10^{-2}. For simulations at $Wa > 1$, the total simulation time was 60, which was sufficient to resolve the difference between near-wall diffusivity and bulk diffusivity. For simulations at $Wa \leq 1$, simulations were carried out for longer (total time of 2160) so as to reduce the variance in the near-wall diffusivity and bulk diffusivity when comparing the two quantities to each other (these two quantities should not differ appreciably in the low-Wa limit).

AUTHOR INFORMATION

Corresponding Author

*E-mail: ngh@mit.edu.

ORCID Ⓘ

Nicolas G. Hadjiconstantinou: 0000-0002-1670-2264

Notes

The authors declare no competing financial interest.

ACKNOWLEDGMENTS

REFERENCES

(1) Hummer, G.; Rasaiah, J. C.; Noworyta, J. P. *Nature* **2001**, *414*, 188−190.
(2) Majumder, M.; Chopra, N.; Andrews, R.; Hinds, B. J. *Nature* **2005**, *438*, No. 44.
(3) Holt, J. K.; Park, H. G.; Wang, Y.; Stadermann, M.; Artyukhin, A. B.; Grigoropoulos, C. P.; Noy, A.; Bakajin, O. *Science* **2006**, *312*, 1034−1037.
(4) Whitby, M.; Quirke, N. *Nat. Nanotechnol.* **2007**, *2*, 87−94.
(5) Wang, G. J.; Hadjiconstantinou, N. G. *Phys. Fluids* **2015**, *27*, No. 052006.
(6) Hahn, K.; Karger, J. *J. Phys. Chem. B* **1998**, *102*, 5766−5771.
(7) Ball, C. D.; MacWilliam, N. D.; Percus, J. K.; Bowles, R. K. *J. Chem. Phys.* **2009**, *130*, No. 054504.
(8) Mittal, J.; Truskett, T. M.; Errington, J. R.; Hummer, G. *Phys. Rev. Lett.* **2008**, *100*, No. 145901.
(9) Mittal, J.; Errington, J. R.; Truskett, T. M. *Phys. Rev. Lett.* **2006**, *96*, No. 177804.
(10) Schoen, M.; Cushman, J. H.; Diestler, D. J.; Rhykerd, C. L., Jr. *J. Chem. Phys.* **1988**, *88*, 1394−1406.
(11) Mittal, J.; Errington, J. R.; Truskett, T. M. *J. Phys. Chem. B* **2007**, *111*, 10054−10063.
(12) Mehdipour, N.; Mousavian, N.; Eslami, H. *J. Iran. Chem. Soc.* **2014**, *11*, 47−52.
(13) Chen, Q.; Moore, J. D.; Liu, Y.-C.; Roussel, T. J.; Wang, Q.; Wu, T.; Gubbins, K. E. *J. Chem. Phys.* **2010**, *133*, No. 094501.
(14) Mashl, R. J.; Joseph, S.; Aluru, N. R.; Jakobsson, E. *Nano Lett.* **2003**, *3*, 589−592.
(15) Striolo, A. *Nano Lett.* **2006**, *6*, 633−639.
(16) Mukherjee, B.; Maiti, P. K.; Dasgupta, C.; Sood, A. K. *ACS Nano* **2010**, *4*, 985−991.
(17) Lee, K.-H.; Sinnott, S. B. *Nano Lett.* **2005**, *5*, 793−798.
(18) Mao, Z.; Sinnott, S. B. *J. Phys. Chem. B* **2000**, *104*, 4618−4624.
(19) Wei, Q.; Bechinger, C.; Leiderer, P. *Science* **2000**, *287*, 625−627.
(20) Golestanian, R. *Phys. Rev. Lett.* **2009**, *102*, No. 188305.
(21) Shukla, A.; Fuchs, R.; Rehage, H. *Langmuir* **2006**, *22*, 3000−3006.
(22) Hinds, B. J.; Chopra, N.; Rantell, T.; Andrews, R.; Gavalas, V.; Bachas, L. G. *Science* **2004**, *303*, 62−65.
(23) Park, S.; Kim, Y.-S.; Kim, W. B.; Jon, S. *Nano Lett.* **2009**, *9*, 1325−1329.
(24) Demontis, P.; Stara, G.; Suffritti, G. *Microporous Mesoporous Mater.* **2005**, *86*, 166−175.
(25) Bocquet, L.; Barrat, J.-L. *Soft Matter* **2007**, *3*, 685−693.
(26) Wang, G. J.; Hadjiconstantinou, N. G. *Phys. Rev. Fluids* **2017**, *2*, No. 094201.
(27) Liu, P.; Harder, E.; Berne, B. J. *J. Phys. Chem. B* **2004**, *108*, 6595−6602.
(28) Allen, M. P.; Tildesley, D. J. *Computer Simulation of Liquids*; Oxford University Press, 1989.
(29) Hansen, J.-P.; McDonald, I. R. *Theory of Simple Liquids*; Elsevier, 2006.
(30) Bocquet, L.; Barrat, J.-L. *Phys. Rev. E* **1994**, *49*, 3079−3092.
(31) Hänggi, P.; Talkner, P.; Borkovec, M. *Rev. Mod. Phys.* **1990**, *62*, 251−341.
(32) Gelb, L. D.; Gubbins, K. E.; Radhakrishnan, R.; Sliwinska-Bartkowiak, M. *Rep. Prog. Phys.* **1999**, *62*, 1573−1659.
(33) Metzler, R.; Jeon, J.-H.; Cherstvy, A. G.; Barkai, E. *Phys. Chem. Chem. Phys.* **2014**, *16*, 24128−24164.
(34) López, E. R.; Pensado, A. S.; Comunas, M. J. P.; Padua, A. A. H.; Fernandez, J.; Harris, K. R. *J. Chem. Phys.* **2011**, *134*, No. 144507.
(35) Heyes, D. M. *J. Chem. Soc., Faraday Trans. 2* **1987**, *83*, 1985−2009.
(36) Barati Farimani, A.; Aluru, N. R. *J. Phys. Chem. B* **2011**, *115*, 12145−12149.
(37) Plimpton, S. *J. Comput. Phys.* **1995**, *117*, 1−19.
(38) Nosé, S. *J. Chem. Phys.* **1984**, *81*, 511−519.
(39) Hoover, W. G. *Phys. Rev. A* **1985**, *31*, 1695−1697.